Carbohydrate Polymers 83 (2011) 171–178

Contents lists available at ScienceDirect

Carbohydrate Polymers

journal homepage: www.elsevier.com/locate/carbpol

Controlled gelation temperature, pore diameter and degradation of a highly porous chitosan-based hydrogel

Qi Feng Dang[a], Jing Quan Yan[b], Jing Jing Li[a], Xiao Jie Cheng[a], Cheng Sheng Liu[a], Xi Guang Chen[a,*]

[a] College of Marine Life Science, Ocean University of China, 5# Yushan Road, Qingdao 266003, PR China
[b] Engineer Research and Development Center of Seabeau Cosmetics Co. Ltd., Qingdao 266111, PR China

ARTICLE INFO

Article history:
Received 28 May 2010
Received in revised form 17 July 2010
Accepted 19 July 2010
Available online 27 July 2010

Keywords:
Highly porous hydrogel
Gelation temperature
Pore diameter
Degradation behavior

ABSTRACT

In this study, highly porous chitosan–α,β-glycerophosphate hydrogels were prepared by changing the chitosan/α,β-glycerophosphate ratio. The gelation temperatures of these gels determined from rheological analysis indicated that the gelation temperature decreased by increasing α,β-glycerophosphate content. The chemical structures and morphology of the hydrogels were examined by FTIR and SEM, respectively. The SEM images showed a highly porous 3D chitosan–α,β-glycerophosphate hydrogel structure with interconnected pores and the pore diameters depended on the chitosan/α,β-glycerophosphate ratio. The swelling and degradation experiments indicated that the degradation behaviors of these hydrogels via bulk erosion relied heavily on the chitosan/α,β-glycerophosphate ratio. This study suggested that the gelation temperature, pore diameter and degradation behaviors of chitosan-based porous hydrogels can be controlled by changing the ratio of chitosan and α,β-glycerophosphate.

1. Introduction

Hydrogels, i.e. polymeric three-dimensional networks able to swell in the presence of an aqueous medium, are widely used in biomedical field as wound dressing (Razzak, Darwis, Zainuddin, & Sukirno, 2001), drug delivery systems (Guo & Gao, 2007; Huang et al., 2009; Zhou et al., 2008), and tissue engineering scaffolds (Dang et al., 2006; Park et al., 2009) because many of their physical properties are similar to natural tissue (Petrini, Farè, Piva, & Tanzi, 2003). The selection of hydrogel is a key factor to the success for all of these applications.

A good candidate for hydrogel formation is chitosan (CS), a non-toxic, biocompatible, and biodegradable material (Rinaudo, 2006). The CS, generally derived from crustaceans, is soluble in acidic media below a pH of 6.5 due to the protonation of the free amine groups on the CS chains (Roberts, 1992). Highly deacetylated semi-diluted CS solutions can be used to formulate homogenous heat-induced hydrogels by neutralizing the solution with a weak base, β-glycerophosphate (β-GP) (Chenite, Buschmann, Wang, Chaput, & Kandani, 2001; Cho, Heuzey, Bégin, & Carreau, 2005a). This in situ gelling hydrogel has the necessary potential to be used as an injectable thermosensitive formulation to encapsulate drugs (Ruel-Gariépy, Chenite, Chaput, Guirguis, & Leroux, 2000; Ruel-Gariépy, Leclair, Hildgen, Gupta, & Leroux, 2002) and cells (Richardson, Hughes, Hunt, Freemont, & Hoyland, 2008). Successful applications of this temperature-responsive hydrogel as an injectable scaffold in angiogenesis, bone repair and cartilage regeneration were discussed by Hou, Bank, and Shakesheff (2004). The characterization of CS-glycerophosphate (CS–GP) hydrogel is very important to the success of such tissue-engineered application. Thus, the general mechanisms of gelation of the CS–GP system have been investigated by Cho et al. (Cho & Heuzey, 2008; Cho, Heuzey, Bégin, & Carreau, 2005a, 2005b; Cho, Heuzey, Bégin, & Carreau, 2006a, 2006b) and Chenite et al. (2001). Jarry Leroux, Haeck, and Chaput (2002) showed that steam sterilization of chitosan solutions induced molecular weight reduction, which leaded to a loss of dynamic viscosity, gelling rate, and mechanical strength of the CS–GP systems. Furthermore, Crompton et al. (2005) examined the morphology and gelation of thermosensitive CS hydrogels with laser scanning confocal microscopy.

Since the CS–GP hydrogels are essentially designed to be used in drug delivery and tissue engineering, rigorous perceptive of their gelation temperature, pore diameter and degradation behaviors may lead to better design of a hydrogel. In this work, the highly porous CS–α,β-GP hydrogels were prepared. The effects of the CS/α,β-GP ratios on the characterizations (such as gelation temperature, gelation time, FTIR, pH value, absorbency and morphology) and degradation behaviors of these kinds of porous hydrogels were investigated. Trypsin was used to investigate the degradation behaviors of these gels in vitro. The interior morphologies of these CS-based porous hydrogels before and after degradation were also observed.

* Corresponding author. Tel.: +86 0532 82032586; fax: +86 0532 82032586.
E-mail address: xgchen@ouc.edu.cn (X.G. Chen).

0144-8617/$ – see front matter © 2010 Elsevier Ltd. All rights reserved.
doi:10.1016/j.carbpol.2010.07.038

2. Materials and methods

2.1. Materials

Chitosan (CS), derived from shrimp shell, dynamic viscosity 140cps, deacetylation degree 96.5%, was freely supplied by Laizhou Haili Biological Product Co., Ltd. (Shandong China). α,β-Glycerophosphate (α,β-GP), lactic acid and Polydimethyl siloxane fluid were all analytical grade (Sigma Co., St. Louis, USA).

2.2. Preparation of CS–α,β-GP hydrogel solutions

Clear solutions of CS (0.18%, w/v) were prepared by dissolving proper amount of CS in aqueous solutions of lactic acid (0.1 M) using a heat collecting magnetic stirrer (DF-1, Beijing Flaming Technology & Trade Co., Ltd. China) at 100 rpm for 8 h at room temperature (25 °C). Then the CS solution was chilled to 4 °C for 30 min. 50% (w/v) aqueous α,β-GP solution was prepared in distilled water and chilled along with the CS solution to 4 °C. Then the α,β-GP solution was added dropwise to the CS solution under stirring and the final CS–α,β-GP solution was mixed for another 30 min. Finally, the resultant CS–α,β-GP hydrogel solutions were stored at 4 °C. The volume of the CS and α,β-GP solutions for each gel was reported in Table 1.

2.3. Gelation temperature

Gelation temperatures for the CS–α,β-GP hydrogel solutions were determined from rheological analysis of the viscoelastic properties of the hydrogel solutions using the Physica MCR101 Rheometer (AnTon paar Ltd., Austria). Polydimethyl siloxane fluid covered the surface of the hydrogel solutions to prevent evaporation during the tests. The effect of the Polydimethyl siloxane fluid on the measurements was shown to be negligible. During the gelation process in non-isothermal conditions, the evolution of rheological properties was investigated between 10 °C and 90 °C using a constant heating rate (2 °C/min). Small amplitude deformation γ (0.02) and low frequency ω (1.00 rad/s) were applied in order not to disturb the gel formation. The gelation temperature (T_{gel}) of the highly porous hydrogel was determined as the crossover of the storage modulus (G') and loss modulus (G'').

2.4. Gelation time

A simple test tube inverting method was employed to determine the gelation time (Chung et al., 2005; Ganji, Abdekhodaie, & Ramazani, 2007). The sol phase was defined as flowing liquid and the gel phase as non-flowing gel when the hydrogel solution in the test tube was inverted. Firstly, 1 mL CS–α,β-GP hydrogel solutions were added into 5 mL tubes with inner diameter of 10 mm and maintained for 12 h at 4 °C to remove air bubbles. The tubes were then incubated in a water bath of proper temperature ($T_{gel} \pm 0.5$ °C) or 37 °C. The gelation time was determined by inverting the tubes every 0.5 min. The time at which the gel did not flow was recorded as the gelation time.

2.5. FTIR, pH value and absorbency kinetics

The infrared spectra of CS, α,β-GP and CS–α,β-GP hydrogels were recorded in KBr pellets on a Nicolet FT-IR 5700 spectrophotometer (Madison, WI, U.S.A.) at room temperature (25 °C) by the method of transmission. Samples of CS–α,β-GP hydrogels were freeze-dried (for 48 h) and triturated before used.

The pH values of the CS–α,β-GP hydrogel solutions were measured using a Delta 320 pH Meter (Mettler Toledo, Greifensee, Switzerland) at 4 °C.

The absorbency kinetics of the CS–α,β-GP hydrogel solutions at 600 nm during the gelation process was studied using a UV-1100 spectrophotometer (UV-1100, Shanghai MAPADA Instruments Co., Ltd. China). The time-dependent absorption at 600 nm was recorded every 10 s at T_{gel} during the sol-to-gel behavior of CS–α,β-GP hydrogel solutions. The temperature was controlled by heat pad (Shanghai Kobayashi Daily Chemical Co., Ltd. China) during the process of the gelation.

2.6. Morphology observation

Hydrogel samples were gelled at T_{gel} and freeze-dried under vacuum for 48 h to maintain the porous structure without any collapse. The interior morphology of CS–α,β-GP porous hydrogel before and after degradation were examined using scanning electron microscopy (KYKY-2800B, Scientific Instrument Co., Ltd. Chinese Academy of Sciences, China).

2.7. Equilibrium swelling ratio of highly porous hydrogels

The classical gravimetric method was used to measure the equilibrium swelling ratios of the hydrogels. The dried gels were immersed into the tri-distilled water or PBS 7.2 at 37 °C and swollen in aqueous medium for 3 days to reach the equilibrium states. The weight of the swollen samples was measured after the excess surface solution had been removed by wet filter paper. Dry gels were weighted after freeze-drying at −50 °C. Taking the average value of three measurements for each sample, and the equilibrium swelling ratio (ESR) was calculated by the following expression:

$$\mathrm{ESR} = \frac{W_s - W_d}{W_d}$$

where W_s and W_d were the weights of the swollen and dried samples, respectively.

2.8. Swelling kinetics of the highly porous hydrogels

The same method as above was used to record the swelling kinetics of the highly porous hydrogels. The dried gels were immersed in tri-distilled water or PBS 7.2 at 37 °C, and the samples were taken out from water or PBS at regular time intervals. After

Table 1
Composite polymer solutions, gelation temperature, pH values, gelation time and equilibrium swelling ratio of S1, S2 and S3 samples.

Composite polymer solutions	Samples	Gelation temperature (°C)	pH value	Gelation time (min)		Equilibrium swelling ratio (%)	
				T_{gel}	37 °C	H_2O	PBS
0.18% CS solution 9.6 ml 50% GP solution 0.4 ml	S1	45.7	6.57	3.0	NG	46.66 ± 2.08	6.87 ± 0.23
0.18% CS solution 9.6 ml 50% GP solution 1.0 ml	S2	35.3	7.11	1.5	1.5	6.43 ± 0.79	6.18 ± 0.15
0.18% CS solution 8.4 ml 50% GP solution 1.6 ml	S3	30.1	7.26	1.5	1	2.66 ± 0.34	4.43 ± 0.14

removing the liquid on the sample surface with wet filter paper, the sample weights were recorded as the average value of three measurements. The swelling ratio (SR) at time t was defined as the following expression:

$$\mathrm{SR} = \frac{W_t - W_\mathrm{d}}{W_\mathrm{d}}$$

where W_t was the weight of the hydrogel at time t and other symbols were the same as defined above.

2.9. Degradation kinetics of the highly porous hydrogels

Degradation of highly porous CS–α,β-GP hydrogels was examined with respect to weight loss under aqueous conditions in the presence of trypsin. Trypsin was dissolved in PBS 7.2 to result in 0.25% (w/v) enzyme solution. CS–α,β-GP hydrogel solutions were placed in water bath (T_gel) for 5 min to allow gelation. Initially dry hydrogels were weighed after quickly frozen at −80 °C and lyophilized at −50 °C (for 48 h). Weight loss of dry hydrogels was monitored as a function of incubation time in enzyme solution at 37 °C. After a predetermined time, the samples were removed from the solution, washed thoroughly with distilled water, and then freeze-dried. The degradation was assessed by measuring the weight loss (%), which was defined as the following expression:

$$\text{Weight loss (\%)} = \frac{W_1 - W_2}{W_1} \times 100$$

Here W_1 and W_2 were the weights of the dry gel before and after degradation, respectively.

3. Results and discussion

3.1. Gelation temperature of the porous hydrogels

The gelation temperature (T_gel) of the CS–α,β-GP hydrogel solutions can be adjusted by combining the different polymers in varying mass ratios (Table 1). The temperature dependence of storage modulus (G') and loss modulus (G'') used to determine T_gel of S1, S2 and S3 CS–α,β-GP hydrogel solutions were shown in Fig. 1. The evolution of the G'' and G'' was investigated in terms of CS/α,β-GP ratios during the heat-induced gelation, using a temperature ramp of 2 °C/min. The storage modulus G' reflected the solid-like component of the rheological behavior, which was thus low at solution stage but increased drastically at the gelation temperature. The T_gel was determined as the temperature at the crossover of the G' and G'' when the G' raised rapidly, and this method had been shown to give an appropriate value of the T_gel (Cho et al., 2005b). The heat-induced gelation could be divided into three regions (see in Fig. 1, S1, S2 and S3): region (1) solution behavior (S1: 10–45.7 °C; S2: 10–35.3 °C; S3: 10–30.1 °C), region (2) fast gelation and region (3) slow gelation. The first region was below T_gel, where G' was lower than G'' for the case of S1 and S3. For the case of S2, the first region was divided two part, which the G' was higher than G'' in the first part following the second part where G' was lower than G''. In the first region of the S1, S2 and S3 samples, the G' and G'' decreased as the temperature increased, showing the common viscoelastic behavior of a liquid. In the second region, G' and G'' increased dramatically with the increase of temperature and G' was higher than G'', indicating that an elastic gel network has formed. The results showed that the T_gel decreased with increasing α,β-GP content (Table 1 and Fig. 1), corresponding to an enhancement of gelation due to an increase of intermolecular interactions and entanglements. The results were similar with that reported in the work of Cho, Heuzey, Begin, and Carreau (2006b).

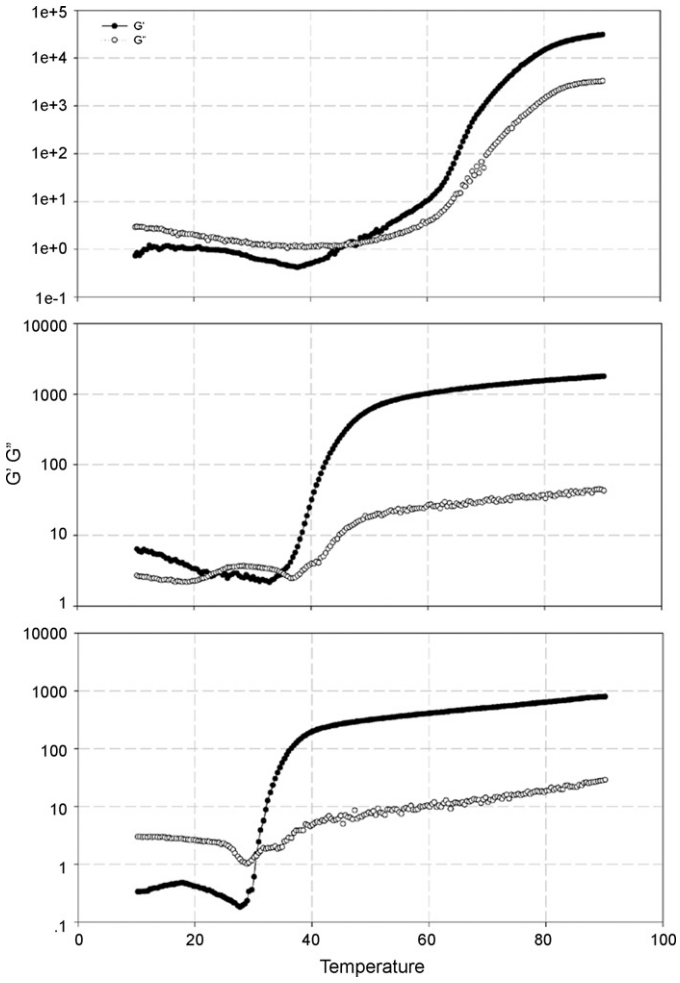

Fig. 1. Loss modulus (G'') and storage modulus (G') of CS–α,β-GP gel solutions as a function of temperature. The crossover points are indicative of gel formation as G' becomes greater than G'' in a certain temperature.

3.2. Gelation time of the porous hydrogels

The gelation time of the CS–α,β-GP porous hydrogels reflected the changes of G' and G'' during the gelation process, indicating the gelation speed. Table 1 gave the gelation time of S1, S2 and S3 hydrogel solutions samples with different CS/α,β-GP ratios at T_gel and 37 °C, respectively. The gels were formed in few minutes when the experiment temperature close to the T_gel. The higher the temperatures, the faster the formation speed of the gel. The influence of CS/α,β-GP ratios on the gelation time, as shown in Table 1, indicated that a decrease of CS/α,β-GP ratio induced a decrease of gelation time. The case of S3 took 1.5 min to become a gel at 30 °C whereas the gelation time of S1 was 3 min at 46 °C. Interestingly, the gelation time was almost the same for S2 at 35.3 °C and S3 at 30.1 °C. But at the same temperature (37 °C), the gelation time of S3 was only 1 min, shorter than the gelation time of S2 (1.5 min).

The effective interactions responsible for the sol/gel transition in CS–α,β-GP hydrogel solutions are supposed as: (1) the CS–GP electrostatic attractions via the ammonium groups of CS and the phosphate moiety of GP salt, (2) hydrogen bonding between the CS chains as a consequence of reduced electrostatic repulsion after neutralization of the CS solution with GP and (3) hydrophobic interactions between CS chains (Chenite et al., 2000; Ruel-Gariépy et al., 2000). At low content of α,β-GP salt, the electrostatic repulsion between glucosamine groups of CS was too much to allow gelation of CS chains. To reduce the positive charge density on CS chains, a

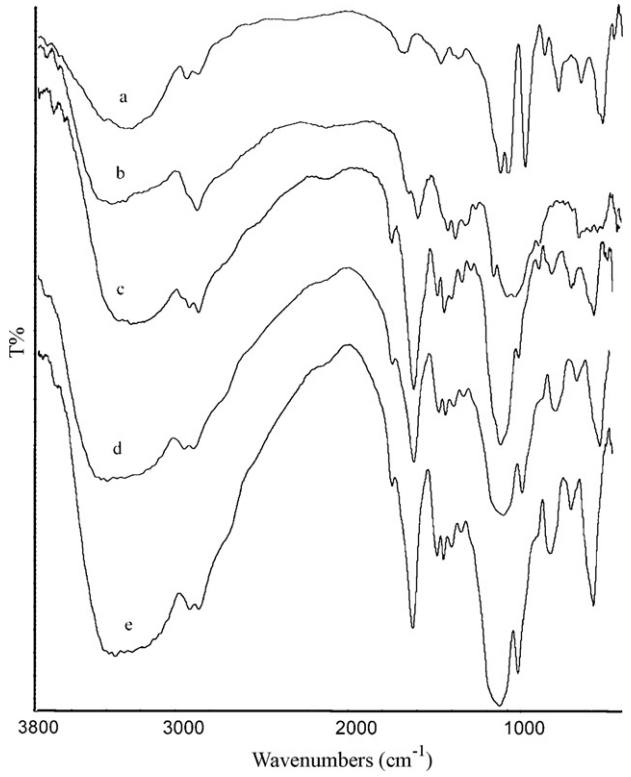

Fig. 2. FT-IR spectra of α,β-GP (a), CS (b) and CS–α,β-GP hydrogels (c): S1; (d) S2; (e) S3.

certain amount of α,β-GP salt was needed. At low CS/α,β-GP ratio, electrostatic attraction between the ammonium groups of CS and the phosphate groups of α,β-GP molecules allowed for extensive hydrogen bonding via OH–NH and O–HN of CS chains. As a result, the gelation time was shorter at lower CS/α,β-GP ratio.

3.3. FTIR, pH value and absorbency kinetics of the porous hydrogels

The differences in chemical structures between the CS, α,β-GP and CS–α,β-GP hydrogels determined by FTIR were shown in Fig. 2. The spectrum of freeze-dried CS–α,β-GP gels had a new peak at 1729 cm^{-1}, which CS and α,β-GP did not have. Moreover, compared with CS, the peaks of the gels at 1596 cm^{-1} (δ N–H of amide II) became stronger and stronger and the peaks at 1322 cm^{-1} (–C–N) become weaker and weaker along with increasing of the α,β-GP content, and the peaks at 1258 cm^{-1} weaken until vanishing along with increasing of the α,β-GP content. The results indicated that CS and α,β-GP had intermolecular interactions during the gelation progress, and the chemical reaction was more obvious when the content of α,β-GP was higher.

The pH values measured at 4 °C for the various hydrogel solutions were reported in Table 1. Increasing α,β-GP content slightly raised the pH due to the neutralizing effect of the phosphate groups of this weak base.

The dynamics curves of absorbency at 600 nm of three different hydrogel solutions during sol-to-gel behavior at T_{gel} were shown in Fig. 3. The results proved the dynamics curves of samples in this work were time dependent at certain temperature. The insets in Fig. 3 demonstrated the appearance of the S2 hydrogels at 0 s, 50 s and 200 s during sol-to-gel behavior at T_{gel}. At 0 s, the S2 sample was milk-white and in the sol state, when the time expanded to 50 s, the S2 sample became transparent and also in the sol state; and at 200 s, the appearance of the S2 was opaque and in the gel

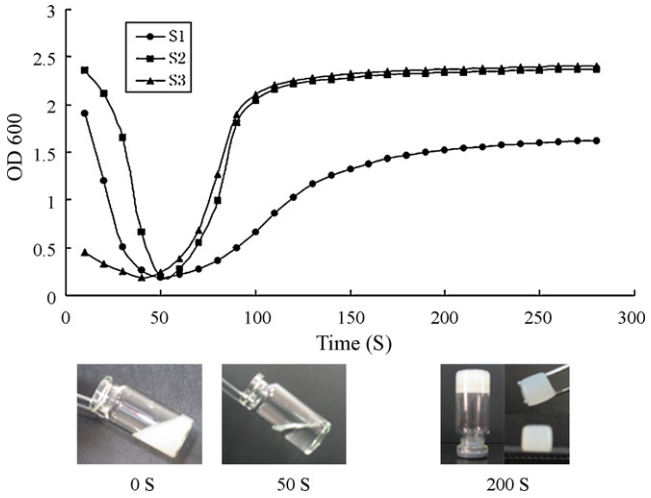

Fig. 3. Dynamics curves of absorbency at 600 nm of S1, S2 and S3 hydrogel during sol-to-gel behavior at T_{gel}. Insets are pictures of S2 hydrogel at 0 s, 50 s and 200 s during the gelation progress.

state. The absorbency of the case of S2 decreased from 2.356 to 0.196 when time expanded from 0 s to 50 s, and then increased rapidly with expanding time. The absorbency at 600 nm could be divided into three regions; after a decreasing region and an afterward rapid increasing region, the absorbency at 600 nm entered a slow increasing region until to achieve stabilization. These three regions could also be intituled: region solution behavior, region fast gelation and region slow gelation. In the high CS/α,β-GP ratio (S1), the absorbency at 600 nm was smaller than samples of low CS/α,β-GP ratio (S3) after gelation, while there was no obvious difference between S1 and S2.

3.4. Morphology observation

The highly porous structure of the hydrogels was studied by means of scanning electron microscopy (SEM). The effects of CS/α,β-GP ratios on the morphology of CS–α,β-GP hydrogels were shown in Fig. 4(a). The interior morphology of all the three hydrogels demonstrated highly porous structure, and the pores formed an interconnecting "open-cell" structure. The structures of channels which formed by pores could make swelling and deswelling fast by water convection. The comparison of the SEM pictures showed the different pore size of three samples, which were caused by changing the ratio of CS and α,β-GP. The pore diameter of the S1 was in the range of 200–500 μm, compared to a diameter of 20–100 μm pores for the S3. This difference in pore size indicated that a lower CS/α,β-GP ratio resulted in the formation of smaller diameters and tighter network structure in porous hydrogels. It can be speculated that varying the CS/α,β-GP ratio could change the pore size in the hydrogel.

3.5. Equilibrium swelling ratio of highly porous hydrogels

The equilibrium swelling ratios (ESR) of the dry hydrogels in water and PBS at 37 °C were indicated in Table 1. All the three samples showed a high ESR in water and PBS 7.2. The case of S1 hydrogel had the highest ESR (46.66 g/g) in water, while the ESR in water of S2 and S3 were 6.43 g/g and 2.66 g/g, respectively. The ESR of the hydrogels in PBS 7.2 was similar in trend comparing to those of water incubation, whereas some differences were found between them. The ESR of S1 hydrogel in PBS 7.2 was 6.87 (g/g, highest of three samples in PBS 7.2), which was significantly lower than 46.66 (g/g) of S1 hydrogel in water. This might because the function of ion in PBS and the PBS 7.2 had higher pH value than tri-distilled water.

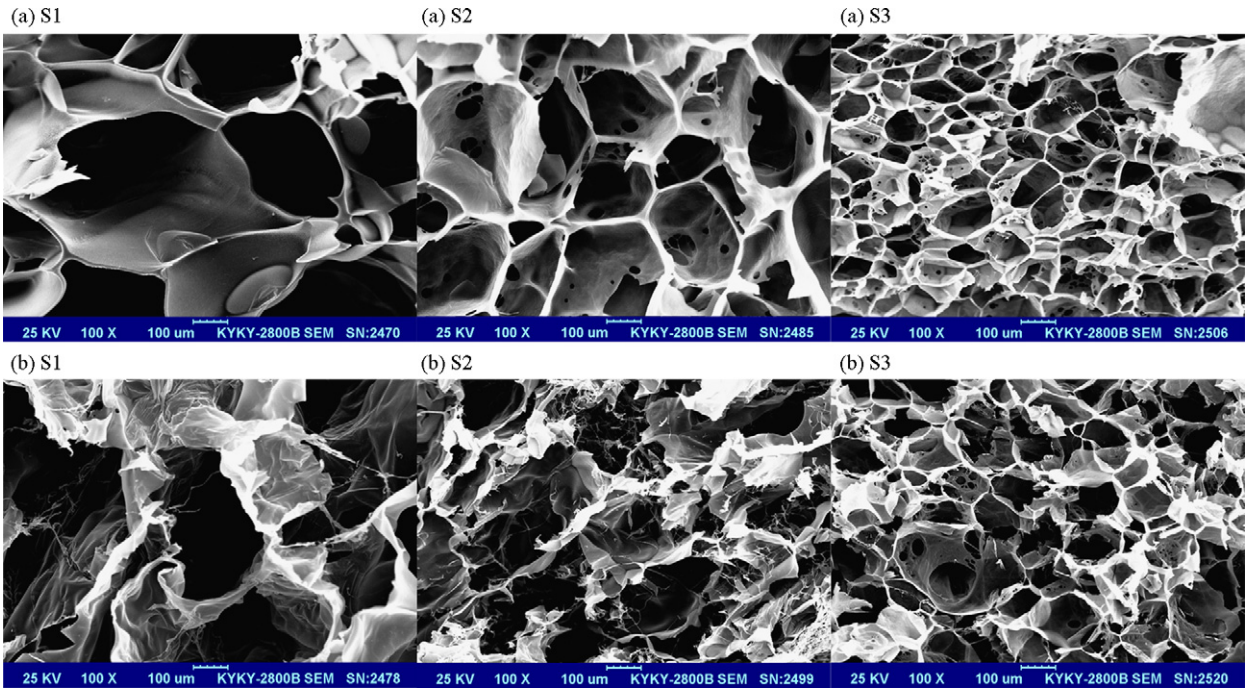

Fig. 4. SEM images to show the internal structures of CS–α,β-GP hydrogels before and after degradation in 0.25% (w/v) trypsin solution at 37 °C. (a) SEM images of the hydrogels before degradation and (b) SEM images of the hydrogels after degradation in trypsin solution at 37 °C for 3 h.

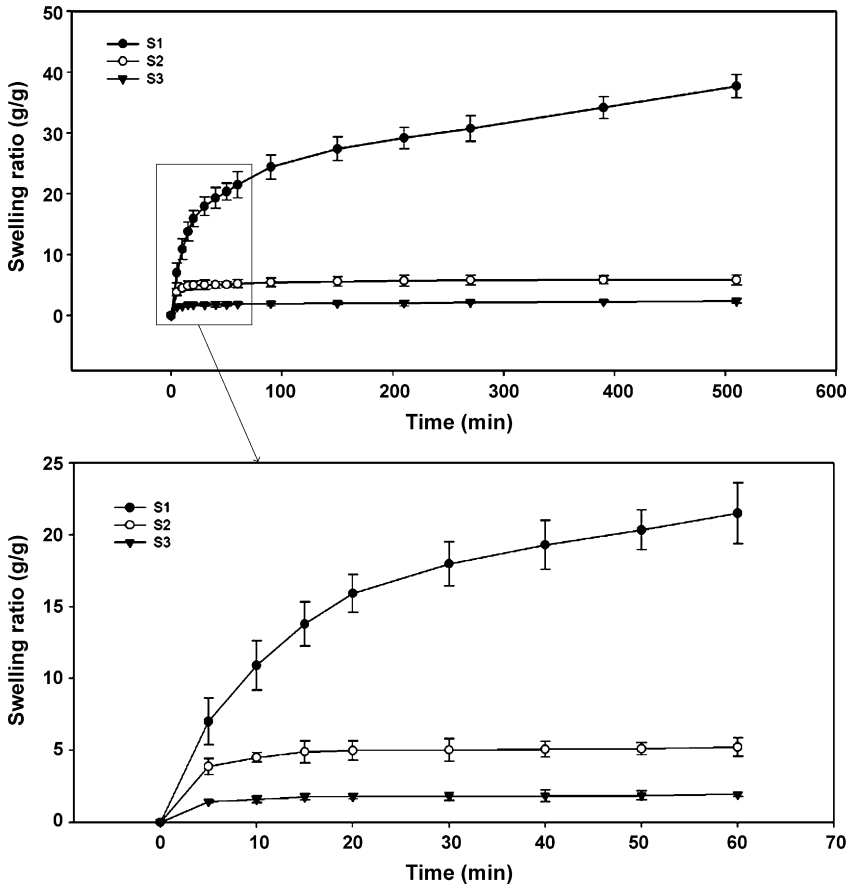

Fig. 5. Swelling kinetics of CS–α,β-GP hydrogels in distilled water at 37 °C.

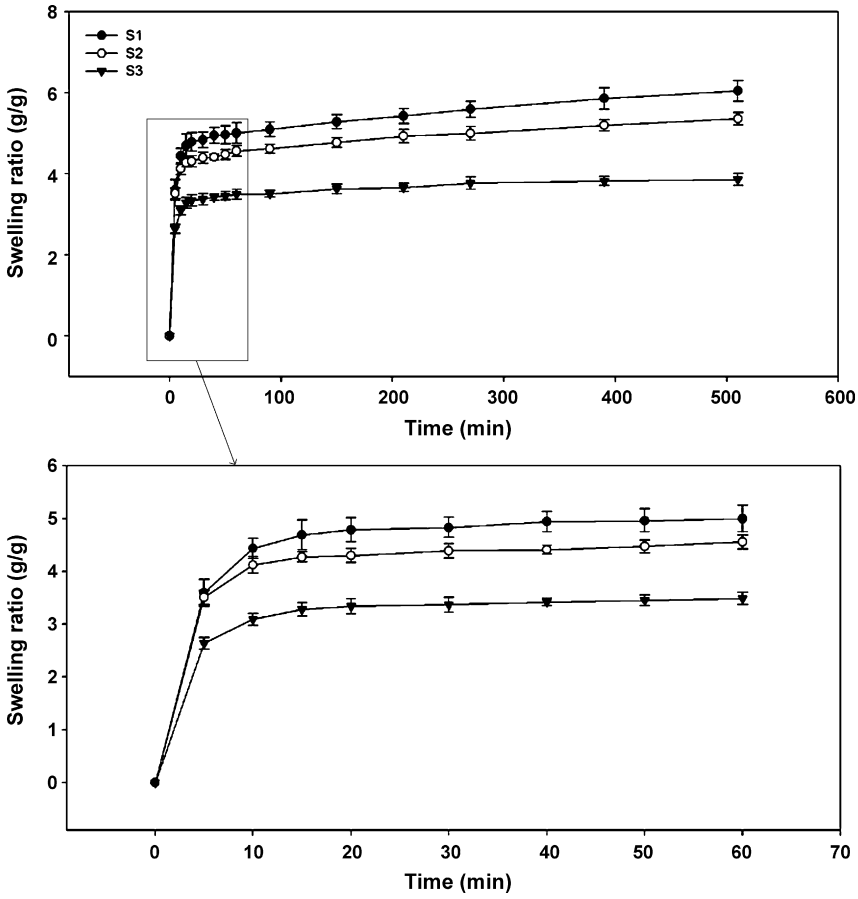

Fig. 6. Swelling kinetics of CS–α,β-GP hydrogels in PBS 7.2 at 37 °C.

The interconnecting and stable internal channel system would enable fast convective water transport inwards or outwards; make possible fast swelling and deswelling by water convection. The swelling characteristics of highly porous hydrogels in water and PBS can be modified by changing the CS/α,β-GP ratio.

3.6. Swelling kinetics of highly porous hydrogels

Figs. 5 and 6 showed the swelling kinetics of the highly porous CS–α,β-GP hydrogels with different CS/α,β-GP ratios in distilled water (Fig. 5) and PBS 7.2 (Fig. 6) at 37 °C, respectively. As expected, a decrease in swelling ratio was seen with a decrease of the ratio of CS and α,β-GP, regardless of the aqueous medium (distilled water or PBS 7.2). The following three steps were proposed to occur in succession during swelling of a dried gel in water (Yoshida et al., 1994): (1) water molecules diffuse into the polymer network; (2) the hydrated polymer chains relax; (3) the polymer network expands into the surrounding liquid. As previous report, hydrogen bonds were formed among the copolymer chains during the formation of the hydrogel (Chen, Du, & Huang, 2003; Wu, Wei, Wang, Su, & Ma, 2007). The hydrogen bond interactions would restrict the movement or relaxation of the gel network chains, and then result in the low swelling rate for copolymer hydrogels (Wang, Feng, Li, & Ruckenstein, 2002). All the three samples (S1, S2 and S3) reached a high swelling equilibrium in a reasonably short time in this work. This might because the channels of "open-cell" pore structures in these hydrogels allowed the solvent to be expelled or absorbed by convection, a much faster process, than by diffusion. The enhanced swelling ratio of sample with lower α,β-GP content in water or PBS 7.2 could be explained by the morphology characteristics of highly porous CS–α,β-GP hydrogels. The SEM images from highly porous CS–α,β-GP hydrogels with different ratios of CS and α,β-GP showed that the size of the pores increased with decreasing α,β-GP content Fig. 4(a). Thus, the swelling ratio for S1 hydrogel by the enhanced porosity should be faster than S3 hydrogel.

3.7. Degradation kinetics of highly porous hydrogels

The degradability of highly porous CS–α,β-GP hydrogels was studied by examining the weight loss and swelling ratio of hydrogels with time in 0.25% (w/v) trypsin solution at 37 °C. Fig. 7(a) showed a typical weight loss curve for degrading CS–α,β-GP hydrogels. The hydrogels showed great increase in the weight loss as a function of time. All the three hydrogels demonstrated a significant weight loss exceeding 60% when the hydrogels incubated in trypsin solution at 37 °C for 1400 min. The weight loss of the gels decreased with increasing of the CS/α,β-GP ratio. For example, as the ratio of CS solution and α,β-GP solution increased from 8.4 ml:1.6 ml (S3) to 9.6 ml:0.4 ml (S1), the degradation after a 1400 min period decreased from 75.48% weight loss to 60.91%. This implied that the degradation of highly porous CS–α,β-GP hydrogels with lower CS/α,β-GP ratio was faster than those with higher CS/α,β-GP ratio, in spite of hydrogels with higher CS/α,β-GP ratio had bigger pores. This result demonstrated that the slower degradation of S1 hydrogel was due to the higher cross-linking density in the hydrogel, which was supported by rheological experiments (Park et al., 2009). The storage modulus G' can be considered as a measure of the extent of gel network formation. The higher G' values of the gel means the stronger gel intensity (Tang, Du, Hu, Shi, & Kennedy, 2007). The hydrogel which had higher cross-linking density had higher stor-

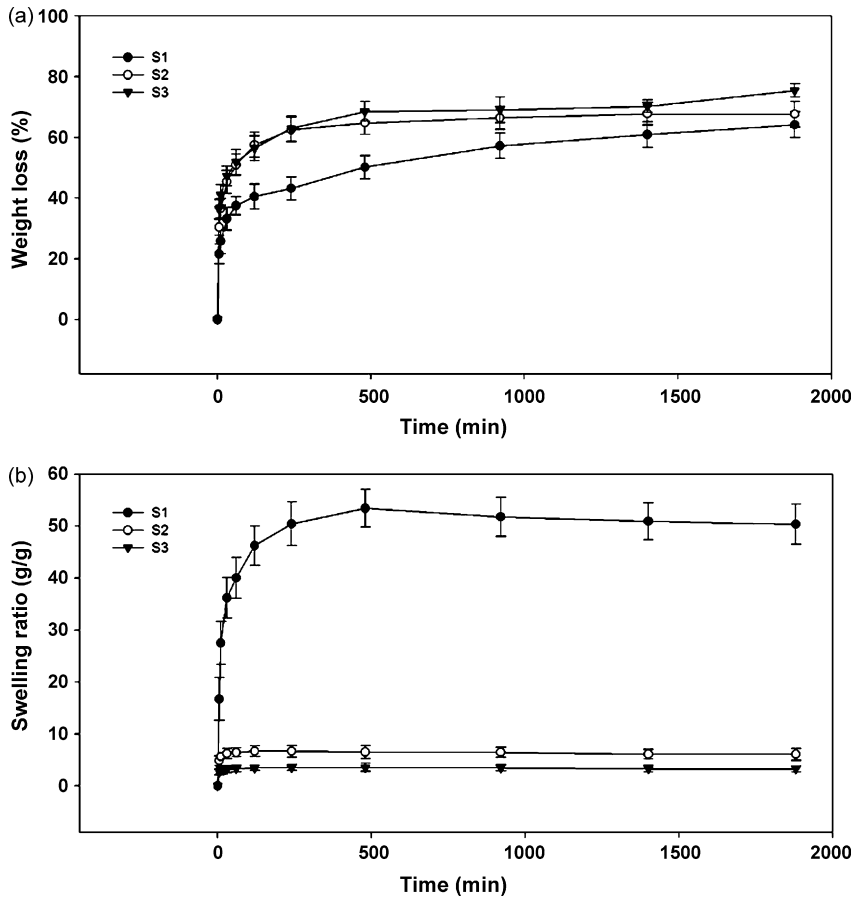

Fig. 7. Degradation kinetics of CS–α,β-GP hydrogels in 0.25% (w/v) trypsin solution at 37 °C. (a) Weight loss (%) of samples during degraded progress and (b) swelling ratio (g/g) of samples during degraded progress.

age modulus. The order of storage modulus from high to low was S1 > S2 > S3, therefore the S1 had highest cross-linking density and lowest degradation rate.

The effect of the CS/α,β-GP ratio on the enzymatic degradation of the hydrogels was also evidenced in SEM images. Fig. 4(b) showed the internal structures of the three samples after 3 h degradation in 0.25% (w/v) trypsin solution at 37 °C. After 3 h degradation, the hydrogels resulted in larger pore diameters, which was likely due to the mass released from the gel matrix. The comparison of the SEM pictures of three hydrogels showed a different morphological structure during enzymatic degradation. The hydrogels with higher CS/α,β-GP ratio had higher cross-linking density, the weight loss of the gels during degradation progress mainly due to the mass released from the gel matrix. When the CS/α,β-GP ratio decreased, besides the mass released, the breaks and fall off of the gel matrix induced the weight loss mainly. Thus the hydrogels with lower CS/α,β-GP ratio had higher degradation rate.

There are two types of degradation processes of hydrogel networks: surface erosion and bulk erosion (Metters, Bowman, & Anseth, 2000). In the process of surface erosion, the water will be adsorbed on the surface before it diffuses into the bulk of the sample, for the rate of water diffusion into a sample is slower than the degraded reaction. Bulk erosion, on the other hand, occurs when the rate of water diffusion into the sample is much faster than the hydrolysis reaction. The interconnecting and stable internal channel system of the highly porous CS–α,β-GP hydrogels in this work would enable fast convective water transport inwards or outwards in these hydrogels. Fig. 7(b) shows that hydrogels in enzyme solution had biggish swelling ratios and the rate of water into a sample by convection, much faster than the diffusion; these facts suggested that the degradation of highly porous CS–α,β-GP hydrogels in aqueous solutions belongs to the bulk-erosion process.

4. Conclusions

The interior morphology of all the three CS–α,β-GP hydrogels prepared in this paper demonstrated highly porous structure, and the pores formed an interconnecting "open-cell" structure. The gelation temperature, pore diameter, equilibrium swelling and enzymatic degradation of the hydrogels were dependent upon the ratios of CS and α,β-GP. The hydrogel with a higher α,β-GP content had lower gelation temperature, smaller pore diameter, lower equilibrium swelling and higher degradation rate. These studies indicated that the thermosensitive highly porous hydrogels could be designed by changing the CS/α,β-GP ratio. This type of highly porous hydrogels with controllable gelation temperature, pore diameter and degradation behavior may have significant advantages for biomedical applications.

References

Chen, L., Du, Y., & Huang, R. (2003). Novel pH, ion sensitive polyampholyte gels based on carboxymethyl chitosan and gelatin. *Polymer International*, *52*, 56–61.

Chenite, A., Buschmann, M., Wang, D., Chaput, C., & Kandani, N. (2001). Rheological characterization of thermogelling chitosan/glycerol–phosphate solutions. *Carbohydrate Polymers*, *46*, 39–47.

Chenite, A., Chaput, C., Wang, D., Combes, C., Buschmann, M. D., Hoemann, C. D., et al. (2000). Novel injectable neutral solutions of chitosan form biodegradable gels in situ. *Biomaterials*, *21*, 2155–2161.

Cho, J., & Heuzey, M. C. (2008). Dynamic scaling for gelation of a thermosensitive chitosan-β-glycerophosphate hydrogel. *Colloid and Polymer Science*, *286*, 427–434.

Cho, J., Heuzey, M. C., Bégin, A., & Carreau, P. J. (2005a). Physical gelation of chitosan in the presence of β-glycerophosphate: The effect of temperature. *Biomacromolecules*, *6*, 3267–3275.

Cho, J., Heuzey, M. C., Bégin, A., & Carreau, P. J. (2005b). Gelation point determination using fast Fourier transform rheometry. In *The society of rheology 77th annual meeting* Vancouver, BC, Canada.

Cho, J., Heuzey, M. C., Bégin, A., & Carreau, P. J. (2006a). Effect of urea on solution behavior and heat-induced gelation of chitosan-β-glycerophosphate. *Carbohydrate Polymers*, *63*, 507–518.

Cho, J., Heuzey, M. C., Bégin, A., & Carreau, P. J. (2006b). Chitosan and glycerophosphate concentration dependence of solution behavior and gel point using small amplitude oscillatory rheometry. *Food Hydrocolloids*, *20*, 936–945.

Chung, H. J., Go, D. H., Bae, J. W., Jung, I. K., Lee, J. W., & Park, K. D. (2005). Synthesis and characterization of Pluronic® grafted chitosan copolymer as a novel injectable biomaterial. *Current Applied Physics*, *5*, 485–488.

Crompton, K. E., Prankred, R. J., Paganin, D. M., Scott, T. F., Horne, M. K., Finkelstein, D. I., et al. (2005). Morphology and gelation of thermosensitive chitosan hydrogels. *Biophysical Chemistry*, *117*, 47–53.

Dang, J. M., Sun, D. D. N., Shin-Ya, Y., Sieber, A. N., Kostuik, J. P., & Leong, K. W. (2006). Temperature-responsive hydroxybutyl chitosan for the culture of mesenchymal stem cells and intervertebral disk cells. *Biomaterials*, *27*, 406–418.

Ganji, F., Abdekhodaie, M. J., & Ramazani, A. S. A. (2007). Gelation time and degradation rate of chitosan-based injectable hydrogel. *Journal of Sol–Gel Science and Technology*, *42*, 47–53.

Guo, B. L., & Gao, Q. Y. (2007). Preparation and properties of a pH/temperature-responsive carboxymethyl chitosan/poly (N-isopropylacrylamide) semi-IPN hydrogel for oral delivery of drugs. *Carbohydrate Research*, *342*, 2416–2422.

Hou, Q., Bank, P. A. D., & Shakesheff, K. M. (2004). Injectable scaffolds for tissue regeneration. *Journal of Materials Chemistry*, *14*, 1915–1923.

Huang, F. Y., Huang, L. K., Lin, W. Y., Luo, T. Y., Tsai, C. S., & Hsieh, B. T. (2009). Development of athermosensitive hydrogel system for local delivery of ^{188}Re colloid drugs. *Applied Radiation and Isotopes*, *67*, 1405–1411.

Jarry, C., Leroux, J. C., Haeck, J., & Chaput, C. (2002). Irradiating or autoclaving chitosan/polyol solutions: Effect on thermogelling chitosan-β-glycerophosphate solutions. *Chemical and Pharmaceutical Bulletin*, *50*, 1335–1340.

Metters, A. T., Bowman, C. N., & Anseth, K. S. (2000). A statistical kinetic model for the bulk degradation of PLA-b-PEG-b-PLA hydrogel networks. *Journal of Physical Chemistry B*, *104*, 7043–7049.

Park, K. M., Lee, S. Y., Joung, Y. K., Na, J. S., Lee, M. C., & Park, K. D. (2009). Thermosensitive chitosan-Pluronic hydrogel as an injectable cell delivery carrier for cartilage regeneration. *Acta Biomaterialia*, *5*, 1956–1965.

Petrini, P., Farè, S., Piva, A., & Tanzi, M. C. (2003). Design, synthesis and properties of polyurethane hydrogels for tissue engineering. *Journal of Materials Science: Materials in Medicine*, *14*, 683–686.

Razzak, M. T, Darwis, D., Zainuddin, & Sukirno. (2001). Irradiation of polyvinyl alcohol and polyvinyl pyrrolidone blended hydrogel for wound dressing. *Radiation Physics and Chemistry*, *62*, 107–113.

Richardson, S. M., Hughes, N., Hunt, J. A., Freemont, A. J., & Hoyland, J. A. (2008). Human mesenchymal stem cell differentiation to NP-like cells in chitosan–glycerophosphate hydrogels. *Biomaterials*, *29*, 85–93.

Rinaudo, M. (2006). Chitin and chitosan: Properties and applications. *Progress in Polymer Science*, *31*, 603–632.

Roberts, G. A. F. (1992). *Chitin chemistry*. Basingstoke, London, Great Britain: The Macmillan Press., pp. 203–206.

Ruel-Gariépy, E., Chenite, A., Chaput, C., Guirguis, S., & Leroux, J. C. (2000). Characterization of thermosensitive chitosan gels for the sustained delivery of drugs. *International Journal of Pharmaceutics*, *203*, 89–98.

Ruel-Gariépy, E., Leclair, G., Hildgen, P., Gupta, A., & Leroux, J. C. (2002). Thermosensitive chitosan-based hydrogel containing liposomes for the delivery of hydrophilic molecules. *Journal of Controlled Release*, *82*, 373–383.

Tang, Y. F., Du, Y. M., Hu, X. W., Shi, X. W., & Kennedy, J. F. (2007). Rheological characterization of a novel thermosensitive chitosan/poly(vinyl alcohol) blend hydrogel. *Carbohydrate Polymers*, *67*, 491–499.

Wang, X. D., Feng, W., Li, H. Q., & Ruckenstein, E. (2002). Optimum toughening via a bicontinuous blending: toughening of PPO with SEBS and SEBS-g-maleic anhydride. *Polymer*, *43*, 37–43.

Wu, J., Wei, W., Wang, L. Y., Su, Z. G., & Ma, G. H. (2007). A thermosensitive hydrogel based on quaternized chitosan and poly (ethylene glycol) for nasal drug delivery system. *Biomaterials*, *28*, 2220–2232.

Yoshida, R., Kaneko, Y., Sakai, K., Okano, T., Sakurai, Y., Bae, Y. H., et al. (1994). Positive thermosensitive pulsatile drug release using negative thermosensitive hydrogels. *Journal of Controlled Release*, *32*, 97–102.

Zhou, H. Y., Chen, X. G., Kong, M., Liu, C. S., Cha, D. S., & Kennedy, J. F. (2008). Effect of molecular weight and degree of chitosan deacetylation on the preparation and characteristics of chitosan thermosensitive hydrogel as a delivery system. *Carbohydrate Polymers*, *73*, 265–273.